

1,3,5-Triazine derivatives as new electron transport–type host materials for highly efficient green phosphorescent OLEDs†

Hsiao-Fan Chen,^a Shang-Jung Yang,^a Zhen-Han Tsai,^b Wen-Yi Hung,^{*b} Ting-Chih Wang^a and Ken-Tsung Wong^{*a}

Received 7th July 2009, Accepted 27th August 2009

First published as an Advance Article on the web 21st September 2009

DOI: 10.1039/b913423a

We have synthesized three star-shaped 1,3,5-triazine derivatives—2,4,6-tris(biphenyl-3-yl)-1,3,5-triazine (**T2T**), 2,4,6-tris(triphenyl-3-yl)-1,3,5-triazine (**T3T**), and 2,4,6-tris(9,9'-spirobifluorene-2-yl)-1,3,5-triazine (**TST**)—as new electron transport (ET)-type host materials for green phosphorescent organic light-emitting devices. The morphological, thermal, and photophysical properties and the electron mobilities of these ET-type host materials are influenced by the nature of the aryl substituents attached to the triazine core. The *meta–meta* linkage between the 1,3,5-triazine core and the peripheral aryl moieties in **T2T** and **T3T** limited the effective extension of their π conjugation, leading to high triplet energies of 2.80 and 2.69 eV, respectively. Time-of-flight mobility measurements revealed the good electron mobilities for these compounds (each $> 10^{-4}$ cm² V⁻¹ s⁻¹), following the order **T3T** > **TST** > **T2T**. The device incorporating **T2T** as the host, doped with (PPy)₂Ir(acac) and 1,3,5-tris(*N*-phenylbenzimidazol-2-yl)benzene (TBPI) as the ET layer, achieved a high external quantum efficiency (η_{ext}) of 17.5% and a power efficiency (η_{p}) of 59.0 lm W⁻¹. For the same device configuration, the **T3T**-based device provided values of η_{ext} and η_{p} of 14.4% and 50.6 lm W⁻¹, respectively; the **TST**-based device provided values of 5.1% and 12.3 lm W⁻¹, respectively. We ascribe the superior performance of the **T2T**-based devices to balanced charge recombination; we ascribe the poor efficiencies of the **TST**-based devices to its relatively low triplet energy (2.54 eV), which did not allow efficient confinement of the triplet excitons on the green phosphorescent emitter (PPy)₂Ir(acac).

Introduction

Phosphorescent light-emitting diodes (PhOLEDs) have attracted considerable attention because they effectively harvest electro-generated singlet and triplet excitons to achieve nearly 100% internal quantum efficiency.¹ The prospective use of PhOLEDs in display and lighting technologies has led to a tremendous amount of research effort being devoted to the development of novel materials and sophisticated device configurations. One strategy toward highly efficient PhOLEDs is to suppress the detrimental effects of transition metal-centered phosphors, such as aggregation quenching and triplet–triplet annihilation, by employing suitable host materials that can accommodate the emitters homogeneously.² Regardless of the emitting colors, the host materials should possess (i) triplet energies higher than those of the guest molecules (to prevent exothermic reverse energy transfer),³ (ii) good charge balance properties (to effectively confine triplet excitons within the emitting layer), (iii) energy levels appropriately aligned with those of the neighboring active layers,

and (iv) decent charge carrier transport properties (to achieve a low operating voltage). In the development of organic materials used for optoelectronics, it is natural to adopt a high-triplet-energy host with preference for hole transport (HT) rather than electron transport (ET). One common example is the use of carbazole-based derivatives,^{3b–c,4} which usually possess high triplet energies and good HT ability.^{4a,5} Thus, most host materials that have been reported previously for use in PhOLEDs exhibiting excellent device characteristics possess the structural features of a carbazole. Progress in the development of ET-type host materials has lagged far behind that of their HT counterparts.

Poor charge carrier mobility and unbalanced charge recombination in the emitting layer are detrimental to the power efficiency of OLEDs.⁶ To improve the carrier drift mobility and achieve good charge balance, ET-type high-triplet-energy host materials with low electron injection barriers, capable of hole-blocking, and high electron mobilities are promising candidates for reducing the operating voltage and improving the device performance. In addition to the triplet energy, suitable thermal stability and energy levels are also critical when designing ET materials. The designed molecules should form morphologically stable and uniform amorphous films when using typical processing techniques. The use of electron-deficient heteroarene-embedded small molecules has proved very useful for improving balanced charge injection and subsequent recombination in OLEDs.⁷ Triazine has an electron affinity (EA) larger than those of other typical electron-deficient heteroaromatic rings (e.g., pyridine, pyrimidine). In addition, it is reasonably

^aDepartment of Chemistry, National Taiwan University, Taipei, 106, Taiwan. E-mail: kenwong@ntu.edu.tw; Fax: +886 2 33661667; Tel: +886 2 33661665

^bInstitute of Optoelectronic Sciences, National Taiwan Ocean University, Keelung, 202. E-mail: wenhung@mail.ntou.edu.tw; Fax: +886 2 24634360; Tel: +886 2 24622192 ext. 6718

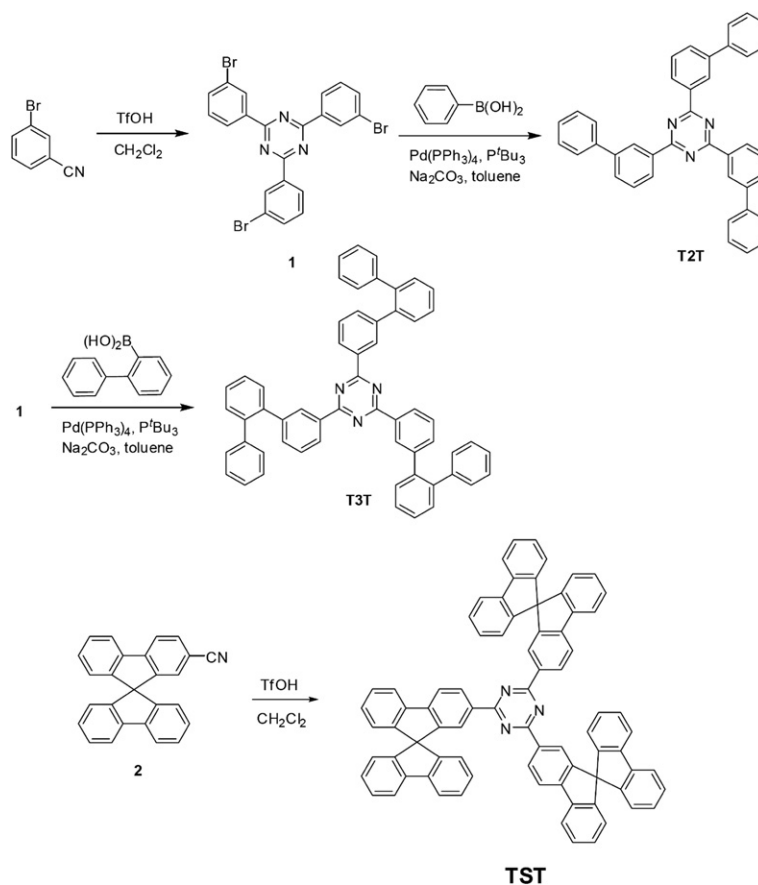
† Electronic supplementary information (ESI) available: Synthetic procedure and spectroscopic characterizations, ¹H, ¹³C NMR spectra of compounds **T2T**, **T3T**, and **TST**; device characteristics of **T2T**, **T3T** and **TST**-based PhOLEDs. See DOI: 10.1039/b913423a

straightforward to structurally modify the 1,3,5-triazine core. As a result, triazine derivatives are electron-deficient heterocycles that are employed widely as active materials in OLEDs.⁸ For example, Pang *et al.* reported that the star-shaped compounds 2,4,6-tris(di-2-pyridylamino)-1,3,5-triazine and 2,4,6-tris[*p*-(di-2-pyridylamino)phenyl]-1,3,5-triazine provide blue emissions when incorporated in electroluminescent devices.⁹ Burn *et al.* observed weak electroluminescence (EL) from a tetrakis(triazine) derivative; a single-layer OLED emitted blue light with an external quantum efficiency (EQE) of 0.003%.¹⁰ Fink *et al.* discovered that the use of dimeric 1,3,5-triazine ethers possessing high glass transition temperatures (T_g) as hole-blocking and ET layers led to increased device efficiency.¹¹ More recently, Kang *et al.* reported a hole- and exciton-blocking material possessing silane and triazine moieties (DTBT) for use in an Ir(PPy)₃-doped CBP device (PPy = phenylpyridine; CBP = 4,4'-bis(*N*-carbazolyl)biphenyl), which exhibited a maximum EQE of 17.5% and a maximum power efficiency of 47.8 lm W⁻¹.¹² Klenker *et al.* reported a triaryl-1,3,5-triazine derivative (BTB) possessing an electron mobility of 7.2×10^{-4} cm² V⁻¹ s⁻¹ at a field of 8×10^5 V cm⁻¹; OLEDs incorporating BTB as the ETL exhibited lower driving voltages and a higher efficiencies relative to those incorporating Alq₃.¹³ Adachi *et al.* established a series of 1,3,5-triazine derivatives (TRZ) as ET-type hosts.^{7c} In particular, the use of 2,4,6-tris(carbazolo)-1,3,5-triazine (TRZ2) as a host for tris(2-phenylpyridine)iridium [Ir(PPy)₃] resulted in an EQE of 10.2% and a power efficiency of 14 lm W⁻¹.

In this paper, we report the syntheses and physical properties of a new series of star-shaped molecules—2,4,6-tris(biphenyl-3-yl)-1,3,5-triazine (**T2T**), 2,4,6-tris(triphenyl-3-yl)-1,3,5-triazine (**T3T**), and 2,4,6-tris(9,9'-spirobifluorene-2-yl)-1,3,5-triazine (**TST**)—and their applications as ET-type host materials in green PhOLEDs. We introduced the various aryl substituents into the triazine core to probe their structure–property relationships. These new ET-type host materials exhibit reasonably high triplet energies (>2.54 eV) and good ET properties ($\mu_e = ca. 10^{-4}$ cm² V⁻¹ s⁻¹), rendering them suitable for hosting green phosphorescent emitters to realize highly efficient, low-driving voltage PhOLEDs. When incorporating typical ET layers [*e.g.*, 1,3,5-tris(*N*-phenylbenzimidazol-2-yl)benzene (TBPI) or 3-(4-biphenyl)-4-phenyl-5-(4-*tert*-butylphenyl)-1,2,4-triazole (TAZ)] to facilitate electron injection and hole blocking, green PhOLEDs featuring **T2T** as the host material provided high EQEs of 17.5% for (PPy)₂Ir(acac) and 17.4% for Ir(PPy)₃. The highly twisted homologue **T3T**, which exhibited superior morphological stability and electron mobility, but a slightly lower triplet energy, served as an effective ET-type host for Ir(PPy)₃, providing a green PhOLED having an EQE of 16.2%.

Results and discussion

Scheme 1 outlines the syntheses of **T2T**, **T3T**, and **TST**. The key intermediate, 1,3,5-tris(3-bromophenyl)triazine (**1**), was synthesized in 83% yield according to a modification of published



Scheme 1 Synthetic routes toward **T2T**, **T3T**, and **TST**.

procedures.¹⁴ We obtained **T2T** and **T3T** in isolated yields of 99 and 98%, respectively, through Suzuki coupling of **1** with phenylboronic acid and biphenyl-2-boronic acid, respectively, in the presence of a catalytic amounts of Pd(PPh₃)₄ and P^tBu₃. We obtained **TST** in 63% yield after treating 2-cyano-9,9'-spirobifluorene (**2**)¹⁵ with a catalytic amount of trifluoromethanesulfonic acid.

We used differential scanning calorimetry (DSC) and thermogravimetric analysis (TGA) to study the morphological properties and thermal stabilities, respectively, of **T2T**, **T3T**, and **TST** (Table 1). Because of their starburst structural features,¹⁶ we observed well-defined glass transition temperatures for **T2T** (95 °C) and **T3T** (108 °C). In addition, no crystallization was evident for **T3T** during the second DSC scan; in contrast, we observed a crystallization peak and a melting peak for **T2T**. For **TST**, there is no distinct phase transition detected up to 400 °C. Compounds **T2T**, **T3T**, and **TST** exhibited good thermal stabilities with decomposition temperatures (T_d , corresponding to 5% weight loss) within the range 352–478 °C. A high glass transition temperature is desirable for host materials in PhOLEDs because it prevents morphological changes and suppresses the formation of aggregates upon heating.

Fig. 1 presents the electronic and photoluminescence (PL) spectra of **T2T**, **T3T**, and **TST** in solution (CH₂Cl₂) and as solid films on a quartz slide. The photophysical data are also summarized in Table 1. **T2T** exhibits a broad absorption band centered at 270 nm in solution and as a solid film. The absorption maximum of **T3T** was slightly red-shifted ($\lambda_{\max} = 275$ nm) because of the three additional peripheral phenyl rings. The dramatically red-shifted absorption maximum of **TST** ($\lambda_{\max} = 355$ nm), relative to those of **T2T** and **T3T**, is consistent with its extended π -conjugation through coplanar fluorene moieties. Compounds **T2T**, **T3T**, and **TST** exhibit deep blue emissions in CH₂Cl₂ solutions with PL peaks located in the range 380–393 nm. The PL spectra of **T2T**, **T3T**, and **TST** in their neat films were slightly red-shifted by 10–20 nm, presumably because of the different dielectric surroundings in the solid state. Fig. 1 displays the phosphorescence spectra of these three ET-type host materials in EtOH at 77 K. We calculated the triplet energies (E_T) of **T2T**, **T3T**, and **TST** to be 2.80, 2.69, and 2.54 eV, respectively; these values are sufficiently high for hosting green phosphorescent emitters, preventing possible reverse energy transfer.

We used photoelectron yield spectroscopy (Riken AC-2) to determine the HOMO energy levels of **T2T**, **T3T**, and **TST**; we estimated the LUMO energy levels from the HOMO values and the optical band gaps (E_g) by using the equation $LUMO = HOMO + E_g$, where the values of E_g of **T2T**, **T3T**, and **TST**, determined from the onset wavelengths of the absorption bands, were 3.56, 3.56, and 3.22 eV, respectively. We calculated the

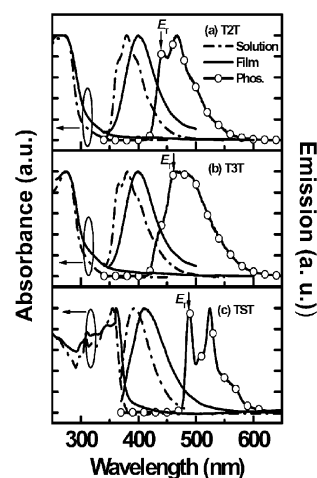


Fig. 1 Room-temperature absorption and emission (PL) spectra of **T2T**, **T3T**, and **TST** in CH₂Cl₂ solutions and as neat films and corresponding phosphorescence (Phos) spectra recorded from their EtOH solutions at 77 K.

corresponding HOMO/LUMO energy levels for **T2T**, **T3T**, and **TST** to be $-5.64/-2.08$ eV, $-5.71/-2.15$ eV, and $-5.69/-2.47$ eV, respectively (Table 1).

We performed time-of-flight (TOF) measurements to evaluate the electron mobilities of **T2T**, **T3T**, and **TST**. Fig. 2(a)–(c) display typical room-temperature TOF transients of electron for these materials under an applied electric field; in each case, we observe dispersive ET behavior. In the double-logarithmic representations [insets to Fig. 2(a)–(c)], the carrier-transit time, t_T , required to determine the carrier mobilities, was extracted from the intersection point of the two asymptotes. In Fig. 2(d), the field-dependent electron mobilities existed in the range from 5×10^{-5} to 9×10^{-4} cm² V⁻¹ s⁻¹ for fields varying from 1.6×10^5 to 5.9×10^5 V cm⁻¹. The observed electron mobility ($\mu_e = ca. 8.7 \times 10^{-4}$ cm² V⁻¹ s⁻¹) of **T3T** was higher than those of **TST** ($\mu_e = ca. 6.8 \times 10^{-4}$ cm² V⁻¹ s⁻¹) and **T2T** ($\mu_e = ca. 1.2 \times 10^{-4}$ cm² V⁻¹ s⁻¹) under the same electric field ($E = 3.6 \times 10^5$ V cm⁻¹). These electron mobilities are similar to those of other 1,3,5-triazine derivatives (e.g., BTB: $\mu_e = ca. 10^{-4}$ cm² V⁻¹ s⁻¹)¹³ and are 10-fold higher than that of the widely used ET material tris(8-hydroxyquinoline) aluminium (Alq₃). The combination of high electron mobilities and reasonably high triplet energy levels for **T2T**, **T3T**, and **TST** indicate that they have potential to serve as ET-type host materials for green PHOLEDs.

To evaluate the ability of the ET-type host materials **T2T**, **T3T**, and **TST** to confine triplet excitons in conjunction with corresponding dopants having values of E_T of less than 2.54 eV,

Table 1 Physical Properties of **T2T**, **T3T**, and **TST**

	$T_g/T_d/T_m$ (°C)	T_d /°C	λ_{abs} /nm [sol./film]	λ_{PL} /nm [sol./film]	E_T /eV	HOMO/LUMO/ E_g^a (eV)	μ_e^b /cm ² V ⁻¹ s ⁻¹
T2T	95/137/204	352	270/270	380/400	2.80	5.64/2.08/3.56	1.2×10^{-4}
T3T	108/ n.d./ n.d.	390	275/275	381/400	2.69	5.71/2.15/3.56	8.7×10^{-4}
TST	N.d./ n.d./ n.d.	478	355/360	393/410	2.54	5.69/2.47/3.22	6.8×10^{-4}

^a HOMO energy level determined using photoelectron yield spectroscopy (AC-2). LUMO = HOMO + E_g ; value of E_g calculated from the absorption onset of the solid film. ^b Value of μ_e determined through TOF measurement at $E = 3.6 \times 10^5$ V cm⁻¹. ^c not detected.

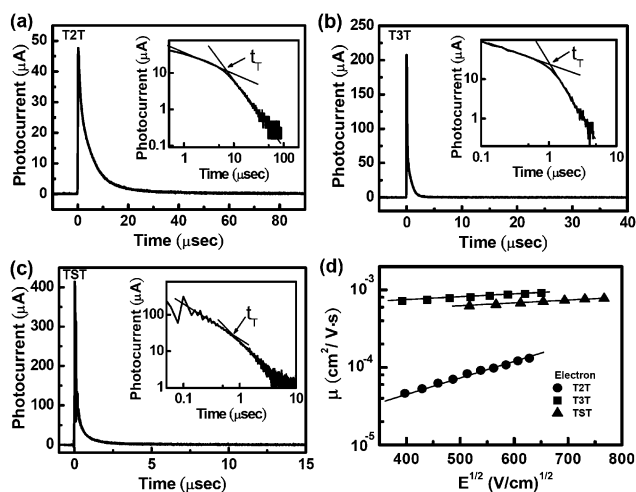


Fig. 2 TOF transients for electrons: (a) **T2T** (thickness: 1.9 μm); $E = 3.2 \times 10^5 \text{ V cm}^{-1}$; (b) **T3T** (thickness: 2.6 μm); $E = 2.7 \times 10^5 \text{ V cm}^{-1}$; (c) **TST** (thickness: 1.87 μm); $E = 3.7 \times 10^5 \text{ V cm}^{-1}$. Insets: Double-logarithmic plots of (a)–(c). (d) Electron mobilities plotted with respect to $E^{1/2}$.

we adopted bis(2-phenylpyridinato)iridium(III) acetylacetonate [(PPy)₂Ir(acac)] and tris(2-phenylpyridinato)iridium(III) [Ir(PPy)₃] as green guests.¹⁷ Initially, we employed a relatively simple four-layer configuration to fabricate the green PHOLED devices: indium tin oxide (ITO)/polyethylene dioxythiophene: poly(styrene sulfonate) (PEDOT:PSS, 30 nm)/4,4'-bis[*N*-(1-naphthyl)-*N*-phenyl]biphenyldiamine (α -NPD, 20 nm)/4,4',4''-tri(*N*-carbazolyl)triphenylamine (TCTA, 5 nm)/1,3,5-triazine derivative:dopant (25 nm)/1,3,5-triazine derivative (50 nm)/LiF (0.5 nm)/Al. Here, we inserted a thin layer of TCTA, which has a high triplet energy ($E_T = ca. 2.76 \text{ eV}$), as an exciton-blocking layer¹⁸ at the α -NPD-1,3,5-triazine derivative interface as a means of preventing exciton diffusion and, hence, resulting in higher device efficiency. LiF and Al served as the electron-injection layer and cathode, respectively. In this device configuration, the 1,3,5-triazine derivative functioned as both host and ET materials. Because triazine derivatives do not exhibit hole-blocking effects, according to the energy level alignments in Fig. 3, and possess high LUMO energies, which could impede electron injection from the cathode, we anticipated that this device configuration might function with relatively high current

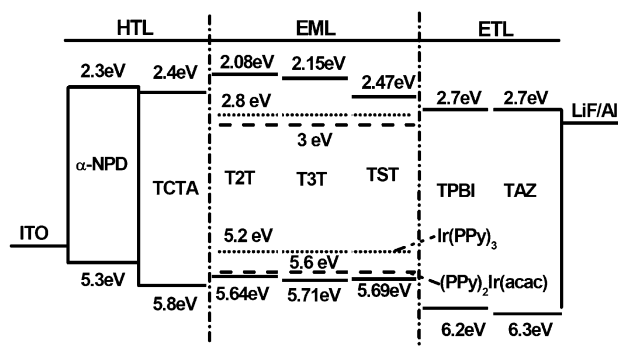


Fig. 3 Energy levels of the HTLs, EMLs, and ETLs used in this study.

leakages and operating voltages, limiting the overall efficiency. To optimize the performance, we also fabricated devices incorporating an additional hole- and exciton-blocking layer of 1,3,5-tris(*N*-phenylbenzimidazo[2-yl]benzene (TPBI)^{4c} or 3-(4-biphenyl)-4-phenyl-5-(4-*tert*-butylphenyl)-1,2,4-triazole (TAZ).¹⁹ The low HOMO/LUMO energy levels of TPBI and TAZ were beneficial for blocking holes and facilitating electron injection/transport, thereby enhancing the device performance (Fig. 3). Table 2 summarizes the electroluminescence data of the devices.

Fig. 4 presents the current density–voltage–luminance (I – V – L) characteristics and EL efficiencies of the devices **A1**–**3** [**T2T** doped with (PPy)₂Ir(acac) and featuring various ET layers (ETLs)]. The I – V and L – V curves of devices **A2** and **A3** feature steep increases, indicating that the TPBI or TAZ layer blocked holes and improved the electron injection/transport properties. Their device performances improved by a factor of 80% with respect to that of device **A1** incorporating **T2T** as the ETL. The best performance was obtained for device **A2** when using TPBI as the ETL; the maximum luminance, external quantum efficiency (η_{ext}), and power efficiency (η_p) were 109,000 cd m^{-2} , 17.5%, and 59 lm W^{-1} , respectively. The value of η_{ext} approaches the theoretical limit of 20% expected for phosphorescence-based OLEDs. At a brightness of 1000 cd m^{-2} , the device efficiency remained high ($\eta_{\text{ext}} = 16\%$ at 5.6 V). We attribute this improved performance to the more-balanced charge flux and better exciton confinement within the emission layer. It appears that the introduction of TPBI as the ET layer and the exciton blocker in this multilayer device reduced the possibility of triplet–triplet annihilation and, therefore, improved the efficiency and reduced the efficiency roll-off.

Device **A3** incorporating TAZ as the ETL exhibited a turn-on voltage of 3 V and a driving voltage of 6.6 V at 1000 cd m^{-2} . We attribute the increased driving voltage, relative to that of device **A2**, to the lower electron mobility of TAZ, leading to lower power efficiency. Device **A3** also exhibited a rather high quantum efficiency of 17.4% and a power efficiency of 48 lm W^{-1} . Fig. 5 presents corresponding EL spectra that reveal a pure green emission arising solely from (PPy)₂Ir(acac), matching perfectly with that reported previously,²⁰ indicating the effective confinement of carriers within the emissive layers. The (PPy)₂Ir(acac)-based green-emitting device using **T2T** as host possesses superior EL performance, particularly in terms of external quantum efficiency (η_{ext}), relative to those of our and other groups' recently reported results (Table 3).

In addition to its (PPy)₂Ir(acac)-based devices, we also used **T2T** as a host material for the Ir(PPy)₃-based devices **B1**–**3** (see Fig. S1 and S2 in the ESI†). The device **B1** incorporating Ir(PPy)₃ as the dopant exhibited higher efficiency ($\eta_{\text{ext}} = 15.7\%$) relative to that of device **A1**. The devices **B2** and **B3** incorporating TPBI and TAZ as ETLs, respectively, also exhibited rather high quantum efficiencies ($\eta_{\text{ext}} = 16.3$ and 15.3%, respectively) and power efficiencies ($\eta_p = 54$ and 47 lm W^{-1} , respectively).

In the series of devices **C** and **D**, we employed **T3T** as the host for the (PPy)₂Ir(acac)- and Ir(PPy)₃-based devices, respectively (see Fig. S3 and S4 in the ESI†). The injection barrier for electrons at the **T3T**–TPBI interface (0.55 eV) was less than that at the **T2T**–TPBI interface (0.62 eV), as indicated in Fig. 3. Furthermore, the observed electron mobility ($\mu_e = ca.$

Table 2 EL Performance of devices as a function of the emitter and ETL

Device	Emitter ^a	ETL	V _{on} ^b /V	1000 nit (V, %)	L _{max} /cd m ⁻²	I _{max} (V)/mA cm ⁻²	η _{ext} (%), cd A ⁻¹	η _p /lm W ⁻¹	CIE1931(x, y)
A1	T2T:	T2T	2.5	10.5, 8.5	49,500	630 (18)	9.7, 36.3	14.7	0.32, 0.64
A2	(PPy) ₂ Ir(acac)	TPBI	2.5	5.6, 16	109,000	1060 (13)	17.5, 56	59	0.33, 0.62
A3	10 wt%	TAZ	3	6.6, 16	85,000	920 (14)	17.4, 54	48	0.32, 0.63
B1	T2T:	T2T	2.5	9.5, 10.1	68,700	690 (17)	15.7, 54	56	0.31, 0.62
B2	Ir(PPy) ₃	TPBI	2.5	5.2, 14.8	97,600	1050 (13)	16.3, 55	54	0.34, 0.61
B3	10 wt%	TAZ	3	5.7, 14.1	97,000	950 (13)	15.3, 52.8	47	0.32, 0.62
C1	T3T:	T3T	2	8, 7.9	90,200	1050 (15.5)	8, 30.3	16.2	0.31, 0.64
C2	(PPy) ₂ Ir(acac)	TPBI	2.5	4.6, 14.1	162,000	1830 (12)	14.4, 53.1	50.6	0.33, 0.63
C3	10 wt%	TAZ	2.5	5.2, 15.7	165,000	1000 (12)	16.2, 62.3	65.2	0.33, 0.63
D1	T3T:	T3T	2.5	8.3, 4.2	34,000	1020 (12)	5.6, 18.4	15.6	0.35, 0.60
D2	Ir(PPy) ₃	TPBI	2.5	4.6, 8	105,000	2000 (10.5)	8.3, 27.2	20.8	0.38, 0.58
D3	10 wt%	TAZ	3	5.2, 8.8	80,600	970 (11)	9.1, 30.1	25.8	0.38, 0.58
E1	TST:	TST	2	7.2, 3.5	44,000	1220 (13)	4, 15.1	10.3	0.36, 0.62
E2	(PPy) ₂ Ir(acac)	TPBI	2.5	5.1, 5	124,000	3400 (11.5)	5.1, 19.4	12.3	0.36, 0.62
E3	10 wt%	TAZ	2.5	5.5, 6.1	84,000	1300 (11.5)	6.1, 23.1	18.9	0.37, 0.61
F1	TST:	TST	2.5	11, 4.2	23,400	780 (19.5)	5.55, 16.6	16.2	0.44, 0.54
F2	Ir(PPy) ₃	TPBI	3	7.5, 5.1	27,600	740 (15)	5.7, 17.1	14.5	0.44, 0.54
F3	10 wt%	TAZ	3.5	8.4, 4.6	31,200	830 (15.5)	5.3, 15.6	12.1	0.44, 0.54

^a Device configuration: ITO/PEDOT:PSS/α-NPD (20 nm)/TCTA (5 nm)/emitter (25 nm)/ETL (50 nm)/LiF (0.5 nm)/Al (100 nm). ^b Turn-on voltage at which emission became detectable (10⁻² cd m⁻²).

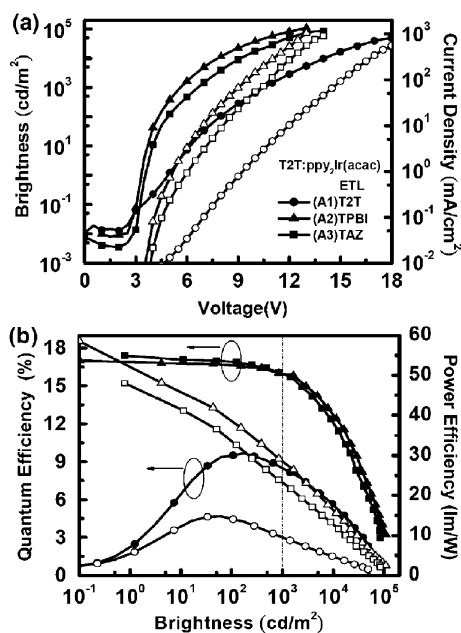


Fig. 4 (a) *I*-*V*-*L* characteristics and (b) plots of EL efficiency versus brightness for devices incorporating T2T doped with (PPy)₂Ir(acac) and featuring various ETLs.

$8.7 \times 10^{-4} \text{ cm}^2 \text{ V}^{-1} \text{ s}^{-1}$) of T3T is higher than that of T2T ($\mu_e = ca. 1.2 \times 10^{-4} \text{ cm}^2 \text{ V}^{-1} \text{ s}^{-1}$) under the same electric field ($E = 3.6 \times 10^5 \text{ V cm}^{-1}$). Thus, the T3T-based devices required lower driving voltages than their corresponding T2T-based devices. The devices C2 and D2 (Table 2) exhibited significantly reduced turn-on voltages (*ca.* 4.6 V) required to reach a luminance of 1000 cd m⁻². In contrast, all of the devices (E and F series) incorporating TST as the host exhibited lower efficiencies and red-shifted emissions in their EL spectra (see Figs. S5 and S6 in the ESI†). We attribute this behavior to the lower triplet energy of TST ($E_T = ca. 2.54 \text{ eV}$), relative to those of T2T and T3T, leading to

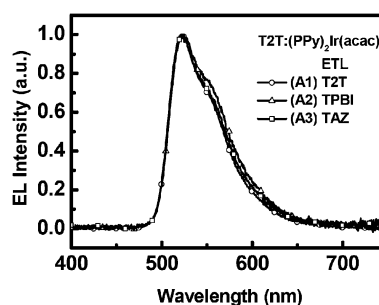


Fig. 5 EL spectra of T2T doped with (PPy)₂Ir(acac) and featuring various ETLs.

Table 3 Performance of recent (PPy)₂Ir(acac)-based green electrophosphorescent devices

Host	Type	L _{max} /cd m ⁻²	η _{ext} (%)	η _p /lm W ⁻¹	Ref.
T2T	ET ^a	109 000 (13 V)	17.5	59	This work
SiInF3	HT ^b	255 000 (9.5 V)	15.8	63	21
T2N	ET	69 000 (17 V)	12.3	38	7e
TPBI-Da	Bipolar	48 400 (16.5 V)	15	70	22
TPBI	ET	78 200	5.7	33	22
CBP	Bipolar	32 500	12.3	38	17
TAZ	ET	—	19	60	23

^a electron-transporting. ^b hole-transporting.

reverse exothermic energy transfer from the guest triplet states to the host, resulting in inefficient triplet energy confinement on the Ir-based emitters within the emissive layers.

Fig. 6 presents the *I*-*V*-*L* characteristics and EL efficiencies of devices incorporating T2T, T3T, and TST as host materials doped with (PPy)₂Ir(acac). The energy levels, triplet energies (E_T), and electron mobilities (see Table 1) of T2T, T3T, and TST affected the device performance dramatically. The *I*-*V* characteristics revealed that the device incorporating T2T as the host

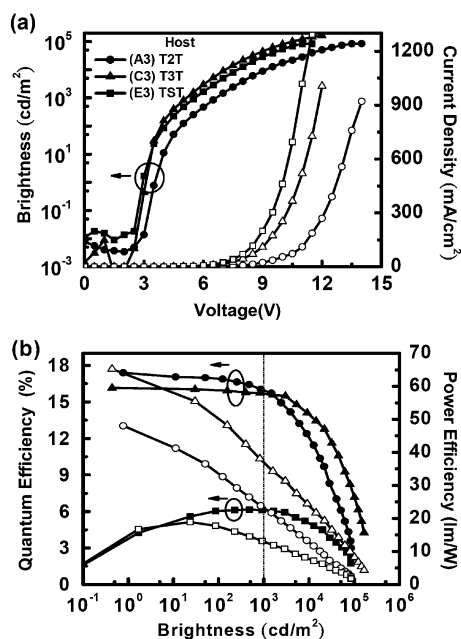


Fig. 6 (a) I - V - L characteristics and (b) plots of EL efficiency versus brightness for host:PPy₂Ir(acac) devices incorporating TAZ as the ETL.

exhibited a slightly lower current density at high voltage relative to those incorporating **T3T** and **TST**, suggesting that **T2T** had a higher energy barrier at the **T2T**-TAZ interface and lower electron mobility ($\mu_e = ca. 10^{-4} \text{ cm}^2 \text{ V}^{-1} \text{ s}^{-1}$). As a result, the hole and electron flows appeared to be better balanced, with electron-hole recombination well-confined within the EML, in the **T2T**-based devices, leading to higher EL efficiency. The device **A3** incorporating **T2T** as the host exhibited the best performance, with maximum values of η_{ext} and η_p of 17.4% and 48 lm W^{-1} , respectively. The highly twisted homologue **T3T**, which possesses superior electron mobility, but slightly lower triplet energy, can serve as an effective ET-type host, providing a green PhOLED exhibiting values of η_{ext} and η_p of 16.2% and 62.3 lm W^{-1} , respectively, for device structure **C3**. The **TST** host possesses extended π -conjugation through its coplanar fluorene moieties, resulting in a relatively low triplet energy ($E_T = ca. 2.54 \text{ eV}$), which could not confine the triplet exciton efficiently because of reverse exothermic energy transfer. We measured the absolute PL quantum efficiency (Φ_{PL}) using a calibrated integration sphere (HAMAMATSU C9920). It was confirmed that a neat film (100 nm) of CBP doped with 10 wt% Ir(PPy)₃ exhibited Φ_{PL} of 64% in our system. The green phosphorescent thin films (100 nm) of **T2T** and **T3T** doped with 10 wt% Ir(PPy)₂(acac) exhibited Φ_{PL} of 52% and 49%, respectively, which are consistent with our observed excellent device efficiencies for devices **A3** ($\eta_{\text{ext}} = 17.4\%$) and **C3** ($\eta_{\text{ext}} = 16.2\%$). In contrast to **T2T** and **T3T**, the thin film (100 nm) of **TST** doped with 10 wt% Ir(PPy)₂(acac) exhibited a rather low Φ_{PL} of 28%, which indicates that the poor capability of **TST** for effectively confining triplet energy of Ir(PPy)₂(acac) due to its relatively lower E_T (2.54 eV). Accordingly, device **E3** exhibited poor device performance, with values of η_{ext} and η_p of 6.1% of 23.1 lm W^{-1} , respectively.

In conclusion, we have synthesized three new star-shaped ET-type host materials, stemming from 1,3,5-triazine cores, for use

in green electrophosphorescent devices. Our molecular design imparted these new host materials with high morphological and thermal stabilities, good electron charge transport properties ($\mu_e = ca. 10^{-4} \text{ cm}^2 \text{ V}^{-1} \text{ s}^{-1}$), appropriate HOMO/LUMO energy levels, and triplet energies suitable for the formation and confinement of excitons in the emitting layer. We employed (PPy)₂Ir(acac) and Ir(PPy)₃ as green emitters dispersed into the ET-type host materials **T2T**, **T3T**, and **TST**. We incorporated various types of ETLs into the following general device configuration: ITO/PEDOT:PSS/ α -NPD (20 nm)/TCTA (5 nm)/host doped with green emitter (25 nm)/ETL (50 nm)/LiF (0.5 nm)/Al (100 nm). In general, the devices incorporating (PPy)₂Ir(acac) as the emitter and TPBI as the ETL exhibited superior efficiencies. Among these three new ET-type host materials, the devices featuring **T2T**, which provided much better balanced electron/hole recombination within the emitting layer, as the host material exhibited superior device characteristics. The best green PhOLED device achieved a high external quantum efficiency of 17.5% and a power efficiency of 65.2 lm W^{-1} .

Experimental

Device fabrication and measurement

All chemicals were purified through vacuum sublimation prior to use. The OLEDs were fabricated through vacuum deposition of the materials at 10^{-6} torr onto ITO-coated glass substrates having a sheet resistance of $15 \Omega \square^{-1}$. The ITO surface was cleaned ultrasonically—sequentially with acetone, methanol, and deionized water—and then it was treated with UV-ozone. The deposition rate of each organic material was $ca. 1\text{--}2 \text{ \AA s}^{-1}$. Subsequently, LiF was deposited at 0.1 \AA s^{-1} and then capped with Al ($ca. 5 \text{ \AA s}^{-1}$) through shadow masking without breaking the vacuum.

The I - V - L characteristics of the devices were measured simultaneously using a Keithley 6430 source meter and a Keithley 6487 picoammeter equipped with a calibration Si-photodiode in a glovebox system. EL spectra were measured using an Ocean Optics spectrometer.

Time-of-flight mobility measurements

The samples for the TOF measurements were prepared through vacuum deposition in the configuration glass/Ag (30 nm)/organic (2–3 μm)/Al (150 nm); they were then placed inside a cryostat and maintained under vacuum. The thickness of the organic film was monitored *in situ* using a quartz crystal sensor and calibrated using a thin film thickness measurement system (K-MAC ST2000). A pulsed nitrogen tunable dye laser was used as the excitation light source (to match the absorption of the organic film) through the semitransparent electrode (Ag)-induced photogeneration of a thin sheet of excess carriers. Under an applied dc bias, the transient photocurrent was swept across the bulk of the organic film toward the collection electrode (Al); it was then recorded using a digital storage oscilloscope. Depending on the polarity of the applied bias, the selected carriers (holes or electrons) were swept across the sample with a transit time of t_T . For an applied bias V and a sample thickness D , the applied electric field E is equal to V/D ; the carrier mobility is then given by the equation

$$\mu = D/(t_T E) = D^2/(Vt_T)$$

from which the carrier transit times, t_T , can be extracted from the intersection points of the two asymptotes to the plateau and tail sections in the double-logarithmic plots.

Acknowledgements

We thank Dr Teng-Chih Chao from Material and Chemical Research Laboratories, Industrial Technology Research Institute (ITRI) for the aid in Riken AC-2 to determine the HOMO energy levels. The work was supported by the financial aid of the National Science Council of Taiwan.

References

- M. A. Baldo, D. F. O'Brien, Y. You, A. Shoustikov, S. Sibley, M. E. Thompson and S. R. Forrest, *Nature*, 1998, **395**, 151.
- S.-J. Su, H. Sasabe, T. I. Takeda and J. Kido, *Chem. Mater.*, 2008, **20**, 1691.
- (a) C. Adachi, R. C. Kwong, P. Djurovich, V. Adamovich, M. A. Baldo, M. E. Thompson and S. R. Forrest, *Appl. Phys. Lett.*, 2001, **79**, 2082; (b) R. J. Holmes, S. R. Forrest, Y.-J. Tung, R. C. Kwong, J. J. Brown, S. Garon and M. E. Thompson, *Appl. Phys. Lett.*, 2003, **82**, 2422; (c) S. Tokito, T. Iijima, Y. Suzuki, H. Kita, T. Tsuzuki and F. Sato, *Appl. Phys. Lett.*, 2003, **83**, 569; (d) K. Goushi, R. Kwong, J. J. Brown, H. Sasabe and C. Adachi, *J. Appl. Phys.*, 2004, **95**, 7798.
- (a) M. A. Baldo, S. Lamansky, P. E. Burrows, M. E. Thompson and S. R. Forrest, *Appl. Phys. Lett.*, 1999, **75**, 4; (b) X. Gong, M. R. Robinson, J. C. Ostrowski, D. Moses, G. C. Bazan and A. J. Heeger, *Adv. Mater.*, 2001, **14**, 581; (c) S.-J. Yeh, M.-F. Wu, C.-T. Chen, Y.-H. Song, Y. Chi, M.-H. Ho, S.-F. Hsu and C.-H. Chen, *Adv. Mater.*, 2005, **17**, 285; (d) K.-T. Wong, Y.-M. Chen, Y.-T. Lin, H.-C. Su and C.-C. Wu, *Org. Lett.*, 2005, **74**, 5361; (e) M.-H. Tsai, H.-W. Lin, H.-C. Su, T.-H. Ke, C.-C. Wu, F.-C. Fang, Y.-L. Liao, K.-T. Wong and C.-I. Wu, *Adv. Mater.*, 2006, **18**, 1216; (f) P.-I. Shih, C.-L. Chiang, A. K. Dixit, C.-K. Chen, M.-C. Yuan, R.-Y. Lee, C.-T. Chen, E. W.-G. Diau and C.-F. Shu, *Org. Lett.*, 2006, **8**, 2799; (g) M.-H. Tsai, Y.-H. Hong, C.-H. Chang, H.-C. Su, C.-C. Wu, A. Matoliukstyte, J. Simokaitiene, S. Grigalevicius, J. V. Grazulevicius and C.-P. Hsu, *Adv. Mater.*, 2007, **19**, 862; (h) D. Tanaka, Y. Agata, T. Takeda, S. Watanabe and J. Kido, *Jpn. J. Appl. Phys.*, 2007, **46**, L117.
- S. Lamansky, P. I. Djurovich, F. Abdel-Razzaq, S. Garon, D. L. Murphy and M. E. Thompson, *J. Appl. Phys.*, 2002, **92**, 1570.
- H. H. Fong, C. H. Wallace Choy, K. N. Hui and Y. J. Liang, *Appl. Phys. Lett.*, 2006, **88**, 113510.
- (a) C. Wang, G. Y. Jung, Y. Hua, C. Pearson, M. R. Bryce, M. C. Petty, A. S. Batsanov, A. E. Goeta and J. A. K. Howard, *Chem. Mater.*, 2001, **13**, 1167; (b) C. J. Tonzola, M. M. Alam, B. A. Bean and S. A. Jenekhe, *Macromolecules*, 2004, **37**, 3554; (c) H. Inomata, K. Goushi, T. Masuko, T. Konno, T. Imai, H. Sasabe, J. J. Brown and C. Adachi, *Chem. Mater.*, 2004, **16**, 1285; (d) S. Oyston, C. Wang, G. Hughes, A. S. Batsanov, I. F. Perepichka, M. R. Bryce, J. H. Ahn, C. Pearson and M. C. Petty, *J. Mater. Chem.*, 2005, **15**, 194; (e) T.-Y. Hwu, T.-C. Tsai, W.-Y. Hung, S.-Y. Chang, Y. Chi, M.-H. Chen, C.-I. Wu, K.-T. Wong and L.-C. Chi, *Chem. Commun.*, 2008, 4956; (f) S. Chen, X. Xu, Y. Liu, W. Qiu, G. Yu, X. Sun, H. Zhang, T. Qi, K. Lu, X. Gao, Y. Liu and D. Zhu, *J. Mater. Chem.*, 2007, **17**, 3788.
- (a) A. P. Kulkarni, C. J. Tonzola, A. Babel and S. A. Jenekhe, *Chem. Mater.*, 2004, **16**, 4556; (b) G. Hughes and M. R. Bryce, *J. Mater. Chem.*, 2005, **15**, 94.
- J. Pang, S. Freiberg, X.-P. Yang, M. D'Iorio and S. Wang, *J. Mater. Chem.*, 2002, **12**, 206.
- J. M. Lupton, L. R. Hemingway, I. D. W. Samuel and P. L. Burn, *J. Mater. Chem.*, 2000, **10**, 867.
- R. Fink, Y. Heischkel, M. Thelakkat and H.-W. Schmidt, *Chem. Mater.*, 1998, **10**, 3620.
- J.-W. Kang, D.-S. Lee, H.-D. Park, Y.-S. Park, J. W. Kim, W.-I. Jeong, K.-M. Yoo, K. Go, S.-H. Kim and J.-J. Kim, *J. Mater. Chem.*, 2007, **17**, 3714.
- R. A. Klenkler, H. Aziz, A. Tran, Z. D. Popovic and G. Xu, *Org. Electron.*, 2008, **9**, 285.
- S. Hayami and K. Inoue, *Chem. Lett.*, 1999, **7**, 545.
- K.-T. Wong, S.-Y. Ku, Y.-M. Cheng, X.-Y. Lin, Y.-Y. Hung, S.-C. Pu, P.-T. Chou, G.-H. Lee and S.-M. Peng, *J. Org. Chem.*, 2006, **71**, 456.
- (a) N. Tamoto, C. Adachi and K. Nagai, *Chem. Mater.*, 1997, **9**, 1077; (b) Z. Gao, C. S. Lee, L. Bello, S. T. Lee, R. M. Chen, T. Y. Luh, J. Shi and C. W. Tang, *Appl. Phys. Lett.*, 1999, **74**, 865; (c) Y. Shirota, K. Okumoto and H. Inada, *Synth. Met.*, 2000, **111**, 387; (d) S. Berleb, W. Brutting, M. Schwoerer, R. Wehrmann and A. Elschner, *J. Appl. Phys.*, 1998, **83**, 4403; (e) K. Itano, T. Tsuzuki, H. Ogawa, S. Appleyard, M. R. Willis and Y. Shirota, *IEEE Trans. Electron Devices*, 1997, **44**, 1218; (f) Y. Kuwabara, H. Ogawa, H. Inada, N. Noma and Y. Shirota, *Adv. Mater.*, 1994, **6**, 677; (g) I. Y. Wu, J. T. Lin, Y. T. Tao and E. Balasubramaniam, *Adv. Mater.*, 2000, **12**, 668; (h) E. Ueta, H. Nakano and Y. Shirota, *Chem. Lett.*, 1994, 2397; (i) Y. Shirota, *J. Mater. Chem.*, 2000, **10**, 25.
- S. Lamansky, P. Djurovich, D. Murphy, F. Abdel-Razzaq, H.-E. Lee, C. Adachi, P. E. Burrows, S. R. Forrest and M. E. Thompson, *J. Am. Chem. Soc.*, 2001, **123**, 4304.
- S.-J. Su, E. Gonmori, H. Sasabe and J. Kido, *Adv. Mater.*, 2008, **20**, 4189.
- J. Kido, M. Kimura and K. Nagai, *Science*, 1995, **267**, 1332.
- C. Adachi, M. A. Baldo, M. E. Thompson and S. R. Forrest, *J. Appl. Phys.*, 2001, **90**, 5048.
- L.-C. Chi, W.-Y. Hung, H.-C. Chiu and K.-T. Wong, *Chem. Commun.*, 2009, 3892.
- S.-Y. Takizawa, V. A. Montes and P. Anzenbacher Jr., *Chem. Mater.*, 2009, **21**, 2452.
- C. Adachi, M. A. Baldo, M. E. Thompson and S. R. Forrest, *J. Appl. Phys.*, 2000, **90**, 5058.